Chapter 1
The Eddy Covariance Method

Thomas Foken, Marc Aubinet, and Ray Leuning

1.1 History

The eddy covariance method for measuring exchanges of heat, mass, and momentum between a flat, horizontally homogeneous surface and the overlying atmosphere was proposed by Montgomery (1948), Swinbank (1951), and Obukhov (1951). Under these conditions, net transport between the surface and atmosphere is one-dimensional and the vertical flux density can be calculated by the covariance between turbulent fluctuations of the vertical wind and the quantity of interest.

Instrumentation limitations hampered early implementation of this approach. In 1949, Konstantinonov (Obukhov 1951) developed a wind vane with two hot wire anemometers to measure the shear stress but the full potential of the eddy covariance method only emerged after the development of sonic anemometers, for which the basic equations were given by Schotland (1955). After the development of the first sonic thermometer (Barrett and Suomi 1949), a vertical sonic anemometer with a 1 m path length (Suomi 1957) was used during the O'Neill experiment in 1953 (Lettau and Davidson 1957). The design of today's anemometers was developed by Bovscheverov and Voronov (1960) and later by Kaimal and Businger (1963) and

T. Foken (✉)
Department of Micrometeorology, University of Bayreuth, 95440 Bayreuth, Germany
e-mail: thomas.foken@uni-bayreuth.de

M. Aubinet
Gembloux Agro-Bio Tech, Unit of Biosystem Physics, University of Liege, 5030 Gembloux, Belgium
e-mail: Marc.Aubinet@ulg.ac.be

R. Leuning
Marine and Atmospheric Research, CSIRO, PO Box 3023, Canberra, ACT 2601, Australia
e-mail: ray.leuning@csiro.au

Mitsuta (1966). These phase shift anemometers have now been replaced by running time anemometers with delay time measurements (Hanafusa et al. 1982; Coppin and Taylor 1983).

Early micrometeorological experiments from the 1950s to 1970s were designed to study fundamental aspects of atmospheric turbulence over homogeneous surfaces, whereas studies in the 1980s investigated the turbulent fluxes of momentum, sensible, and latent heat over heterogeneous surfaces. Similar experiments were conducted in the United States (FIFE, Sellers et al. 1988), in France (HAPEX, André et al. 1990), and in Russia (KUREX, Tsvang et al. 1991). These experiments were to become the basis of many further micrometeorological experiments (Foken 2008) that needed researchers who were highly experienced in micrometeorology and sensor handling.

The possibility of continuous eddy flux measurements arose in the 1990s with the development of a new generation of sonic anemometers (see reviews by Zhang et al. 1986; Foken and Oncley 1995) and infrared gas analyzers for water vapor and carbon dioxide, together with the first comprehensive software packages for the eddy covariance method (McMillen 1988). In the early 1990s, the eddy covariance method became more and more widely used by the ecological community for the measurement of the carbon dioxide and water exchange between an ecosystem and the atmosphere. The first measuring towers of what later became the international FLUXNET network (Baldocchi et al. 2001) were installed, and introductions into techniques new for nonmicrometeorologists were written (Aubinet et al. 2000; Moncrieff et al. 1997a, b). In parallel, the development of new analyzer types allowed an extension of the investigated trace gas spectrum. In particular, Tunable Diode Laser and Quantum Cascade Laser spectrometers were used for the measurement of methane and nitrous oxide (Smith et al. 1994; Laville et al. 1999; Hargreaves et al. 2001; Kroon et al. 2010), Proton Transfer Reaction Mass Spectrometers for volatile organic compounds (Karl et al. 2002; Spirig et al. 2005), and Chemiluminescent sensors for Ozone (Güsten and Heinrich 1996; Gerosa et al. 2003; Lamaud et al. 1994, a.o.).

Some milestones in the development of the eddy covariance method are given in Table 1.1 with the reference to the Chapters of this book.

1.2 Preliminaries

1.2.1 Context of Eddy Covariance Measurements

Eddy covariance measurements are typically made in the surface boundary layer, which is approximately 20–50 m high in the case of unstable stratification and a few tens of meters in stable stratification (see Stull 1988; Garratt 1992; Foken 2008; for complete definitions of layers in the atmosphere). Fluxes are approximately constant with height in the surface layer; hence measurements taken in this layer

Table 1.1 History of the development of the eddy covariance method

Historical milestone	References	See chapter/ section
Theoretical basis of the eddy covariance method	Montgomery (1948), Swinbank (1951), Obukhov (1951)	Section 1.2
Three-dimensional sonic anemometer	Bovscheverov and Voronov (1960), Kaimal and Businger (1963), Mitsuta (1966)	Chapter 2
Instrumental requirements	McBean (1972)	Chapter 2
Gas analyzer for water vapor (UV)	Buck (1973), Kretschmer and Karpovitsch (1973), Martini et al. (1973)	
Gas analyzer for water vapor (IR)	Elagina (1962), Hyson and Hicks (1975), Raupach (1978)	Chapter 2
Correction of the effect of the air density	Webb et al. (1980)	Section 4.1
Gas analyzer for carbon dioxide (IR)	Ohtaki and Matsui (1982), Elagina and Lazarev (1984)	Chapter 2
Transformation of buoyancy flux into sensible heat flux	Schotanus et al. (1983)	Section 4.1
System of transfer functions for spectral correction	Moore (1986)	Section 4.1
Fetch conditions	Gash (1986)	Chapter 8
Real-time data processing software	McMillen (1988)	Chapter 3
Source regions for fluxes (footprint), based on Gash (1986)	Schmid and Oke (1990), Schuepp et al. (1990)	Chapter 8
Relaxed eddy accumulation method, based on Desjardins (1977)	Businger and Oncley (1990)	
Influence of tubing of closed path sensors	Leuning and Moncrieff (1990)	Section 4.1.3 Chapter 3
Theoretical basis for flux footprints and sampling strategies	Horst and Weil (1994), Lenschow et al. (1994)	Chapter 8
Addressing the problem of the unclosed energy balance at the surface	Foken and Oncley (1995)	Section 4.2
Quality tests for eddy covariance data	Foken and Wichura (1996), Vickers and Mahrt (1997)	Section 4.3
Addressing the problem of vertical advection	Lee (1998) and many others	Section 1.3, Chapter 5
Methodology for FLUXNET network (EuroFlux)	Aubinet et al. (2000)	All chapters
Gap filling in the FLUXNET network	Falge et al. (2001a, b)	Chapter 6
Organization of an international network (FLUXNET)	Baldocchi et al. (2001)	All chapters

Foken et al. (1995), Foken (2008), Moncrieff (2004), modified

are representative of the fluxes from the underlying surfaces which are desired to be known. Here atmospheric turbulence is the dominant transport mechanism, justifying the use of the eddy covariance approach to measure the fluxes.

Some preliminary definitions are necessary before discussing the eddy covariance approach in detail.

1.2.2 Reynolds Decomposition

The description of turbulent motions in the following theory sections requires the decomposition of the time-series of each variable ζ into a time-mean part, $\bar{\zeta}$, and a fluctuating part, ζ', the so-called Reynolds decomposition (Fig. 1.1). This can be written as:

$$\zeta = \bar{\zeta} + \zeta' \tag{1.1a}$$

where:

$$\bar{\zeta} = \frac{1}{T} \int_{t}^{t+T} \zeta(t)dt \tag{1.1b}$$

The application of Reynolds decomposition requires some averaging rules for the turbulent value ζ' which are termed Reynolds postulates:

$$
\begin{aligned}
&\text{I} \quad \overline{\zeta'} = 0 \\
&\text{II} \quad \overline{\zeta\xi} = \bar{\zeta}\bar{\xi} + \overline{\zeta'\xi'} \\
&\text{III} \quad \overline{\bar{\zeta}\xi} = \bar{\zeta}\bar{\xi} \\
&\text{IV} \quad \overline{a\zeta} = a\bar{\zeta} \\
&\text{V} \quad \overline{\zeta + \xi} = \bar{\zeta} + \bar{\xi}
\end{aligned}
\tag{1.2}
$$

where a is a constant.

Stricto sensu, these relations are valid only when averages are by "ensemble" averaging (i.e., averaging over many realizations under identical conditions, Kaimal and Finnigan 1994). However, this is never possible in atmospheric measurements, so averages are most often computed on the basis of time series of statistical quantities by making use of the ergodic hypothesis which states that time averages are equivalent to ensemble averages (Brutsaert 1982; Kaimal and Finnigan 1994). To fulfil this assumption, the fluctuations have to be statistically stationary during the averaging time chosen (see Chap. 4).

Fig. 1.1 Schematic presentation of Reynolds decomposition of the value ζ (Foken 2008)
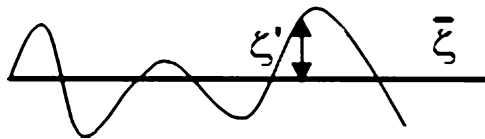
1.2.3 Scalar Definition

The following variables are commonly used in the literature (and throughout this book) to define the scalar intensity of an atmospheric constituent s: *density* (ρ_s, kg m^{-3}) and *molar concentration* (c_s mol m^{-3}) represent the mass and the number of moles of s per volume of air, respectively. The *mole fraction* (mole mole^{-1}) is the ratio of the moles of s divided by the total number in the mixture (also equal to the ratio of the constituent partial pressure to the total pressure), the *molar mixing ratio* ($\chi_{s,m}$, mole mole^{-1}) is the ratio of the constituent mole number to those of dry air, and the *mass mixing ratio* (χ_s, kg kg^{-1}) is the ratio of the mass of the constituent to the mass of dry air. These variables are related by the perfect gas and the Dalton laws.

However, among these variables, only the molar and mass mixing ratios are conserved quantities in the presence of changes in temperature, pressure, and water vapor content (see Kowalski and Serrano-Ortiz (2007) for a more complete discussion). Unfortunately, the variables that are directly measured in the field by infrared gas analyzers are rather density and molar concentration, quantities that are not conserved during heat conduction, air compression/expansion or evaporation, and water vapor diffusion. Therefore, variations in these quantities may appear even in the absence of production, absorption, or transport of the component. The corrections that are necessary to take these effects into account were extensively discussed by Webb et al. (1980) and reexamined by Leuning (2003, 2007). They will be presented in Sect. 4.1.4.

The conservation equations developed in the section below are written using the mass mixing ratio but, for convenience, the other variables will also appear in this book. Conversion factors of one variable into another are given in Table 1.2.

Table 1.2 Conversion factors between different variables characterizing scalar intensity

Conversion factor	Molar mixing Ratio, $\chi_s=$	Mass mixing Ratio, $\chi_{sm}=$	Molar concentration, $c_s=$	Density, $\rho_s=$
Molar mixing ratio, χ_s X	1	$\dfrac{m_s}{m_d}$	$\dfrac{p_d}{R\,\overline{\theta}}$	$\dfrac{m_s\,p_d}{R\,\overline{\theta}}$
Mass mixing Ratio, χ_{sm} X	$\dfrac{m_d}{m_s}$	1	$\dfrac{m_d\,p_d}{m_s\,R\,\overline{\theta}}$	$\dfrac{m_d\,p_d}{R\,\overline{\theta}}$
Molar concentration, c_s X	$\dfrac{R\,\overline{\theta}}{p_d}$	$\dfrac{m_s\,R\,\overline{\theta}}{m_d\,p_d}$	1	m_s
Density, ρ_sX	$\dfrac{R\,\overline{\theta}}{m_s\,p_d}$	$\dfrac{R\,\overline{\theta}}{m_d\,p_d}$	$\dfrac{1}{m_s}$	1

Note that p_d corresponds to the dry air pressure (namely $p - p_v$). As a result, the exact conversion of mass or molar mixing ratio into concentration or density needs the knowledge of water vapor pressure (for details see list of symbols)

1.3 One Point Conservation Equations

The equation describing the conservation of any scalar or vector quantity ζ in the atmosphere may be written as

$$\underbrace{\frac{\partial \rho_d \zeta}{\partial t}}_{I} + \underbrace{\vec{\nabla}(\vec{u}\rho_d \zeta)}_{II} + \underbrace{K_\zeta \Delta(\rho_d \zeta)}_{III} = \underbrace{S_\zeta}_{IV} \tag{1.3}$$

where $\vec{u}$ is the wind velocity vector, $\vec{\nabla}$ and Δ represent the divergence $\left(\frac{\partial}{\partial x}, \frac{\partial}{\partial y}, \frac{\partial}{\partial z}\right)$ and Laplacian $\left(\frac{\partial^2}{\partial x^2} + \frac{\partial^2}{\partial y^2} + \frac{\partial^2}{\partial z^2}\right)$ operators, ρ_d is the dry air density, K_ζ is the molecular diffusivity of the quantity ζ, and S_ζ represents its source/sink strength. This equation is instantaneous and applies to an infinitesimal volume of air. It states that the *rate of change of the quantity* (I) can be due to its *atmospheric transport* (II) to *molecular diffusion* (III) or to its *production by a source/absorption by a sink* into the infinitesimal volume (IV). It can be applied to any scalar or vector quantity provided source terms are defined accordingly. In particular, if ζ is 1, Eq. 1.3 is the continuity equation, if ζ is air enthalpy, it is the enthalpy conservation equation, and if ζ is the mixing ratio of an atmospheric component (water vapor, carbon dioxide, etc.), it is the scalar conservation equation. If the quantity is a component of the velocity vector in one given direction, Eq. 1.3 expresses the conservation of the momentum component in this direction. The three equations describing the momentum conservation in the three directions constitute the Navier Stokes equations.

Application of these equations to the surface boundary layer requires application of the Reynolds decomposition rules: the variables ζ, ρ_d, $\vec{u}$, and S_ζ should each be decomposed into a mean and a fluctuating part according to Eq. 1.1, followed by application of the averaging operator, and appropriate rearrangement and simplification. This procedure will be applied to each equation below.

1.3.1 Dry Air Mass Conservation (Continuity) Equation

By replacing ζ by 1 in Eq. 1.3, one obtains

$$\frac{\partial \rho_d}{\partial t} + \vec{\nabla}(\vec{u}\rho_d) = 0 \tag{1.4}$$

as there is neither a source nor sink of dry air in the atmosphere. Application of the time- averaging operator gives immediately:

$$\overline{\frac{\partial \rho_d}{\partial t}} + \vec{\nabla}(\overline{\vec{u}\rho_d}) = 0 \tag{1.5}$$

1.3.2 Momentum Conservation Equation

By replacing ζ in Eq. 1.3 with the component of wind velocity in one given direction, u_i, one obtains the momentum conservation equation in this direction:

$$\frac{\partial \rho_d u_i}{\partial t} + \vec{\nabla}(\vec{u} \rho_d \, u_i) = S_i \tag{1.6}$$

In Eq. 1.6, the source/sink terms correspond to momentum source/sink, namely to forces. Forces that can act on air parcels in the atmospheric boundary layer are drag, pressure gradient, Coriolis forces, viscous forces, or buoyancy. The first three forces are considered negligible for a flat, horizontally homogeneous surface boundary layer above the roughness elements (i.e. not including vegetation) (Businger 1982; Foken 2008; Stull 1988). Buoyancy appears only in the equation for vertical momentum. The horizontal component of momentum parallel to the mean wind is dominant in the surface boundary layer and thus the buoyancy term is not considered. In a Cartesian coordinate system (x, y, z) where x corresponds to the horizontal, parallel to the average wind velocity, y to the horizontal, perpendicular to the average velocity, and z to the vertical; u, v, w are the x, y, and z components of velocity, respectively, and this equation is written as

$$\frac{\partial \rho_d u}{\partial t} + \frac{\partial \rho_d u^2}{\partial x} + \frac{\partial \rho_d vu}{\partial y} + \frac{\partial \rho_d wu}{\partial z} = 0 \tag{1.7}$$

Application of the Reynolds decomposition to Eq. 1.7 and use of the following simplifications (Businger 1982; Stull 1988):

$$I \quad \left| p'/\bar{p} \right| \ll \left| \rho'_d / \overline{\rho_d} \right|$$

$$II \quad \left| p'/\bar{p} \right| \ll \left| \theta'/\bar{\theta} \right|,$$

$$III \quad \left| \rho'_d / \overline{\rho_d} \right| \ll 1$$

$$IV \quad \left| \theta'/\bar{\theta} \right| \ll 1 \tag{1.8}$$

where p is the pressure and θ the air temperature, leads to

$$\frac{\overline{\partial u}}{\partial t} + \bar{u}\frac{\partial \bar{u}}{\partial x} + \bar{v}\frac{\partial \bar{u}}{\partial y} + \bar{w}\frac{\partial \bar{u}}{\partial z} + \frac{\partial \overline{u'^2}}{\partial x} + \frac{\partial \overline{v'u'}}{\partial y} + \frac{\partial \overline{w'u'}}{\partial z} = 0 \tag{1.9}$$

Equation 1.8, III corresponds to the *Boussinesq-approximation* (Boussinesq 1877), which neglects density fluctuations except in the buoyancy (gravitation) term, because the acceleration of gravity is relatively large in comparison with the other accelerations in the momentum equation. By choosing a coordinate system such that

$\bar{v}$ and $\bar{w}$ are zero and assuming *horizontal homogeneity* (horizontal gradients nullify) and *steady state conditions* (time derivative nullifies) we obtain finally

$$\frac{\partial \overline{w'u'}}{\partial z} = 0 \tag{1.10}$$

Where $\overline{w'u'}$ is the *eddy covariance* term. Equation 1.10 suggests that, under the preceding assumptions, this flux is constant with height and that it is representative of the vertical flux of momentum through a horizontal plane above the surface roughness elements. This approach is called the *eddy covariance method*.

Neglecting the *pressure gradient*, *molecular/viscous transport*, *gravity*, and *Coriolis* terms to derive Eq. 1.10 does not have significant impact on the eddy covariance method over flat, homogeneous surfaces. These conditions are however rare in ecosystems located in a patchy landscape or undulating topography. *Steady-state conditions* are also rare in the surface layer because of diurnal variations in atmospheric stability. It is then necessary to measure the change in storage term using an array of sensors (Sect. 2.5) or to assume quasi-steady conditions. Methods to estimate errors caused by neglecting the storage term are included in the data quality procedures discussed in Sect. 4.3.

1.3.3 Scalar Conservation Equation

By replacing ζ in Eq. 1.3 by χ_s, the mixing ratio of one atmospheric component, one obtains

$$\frac{\partial \rho_d \chi_s}{\partial t} + \vec{\nabla}(\vec{u}\rho_d \chi_s) = S_s \tag{1.11}$$

Through application of the Reynolds decomposition and the continuity Eq. 1.5, Leuning (2003) showed that Eq. 1.11 can be written as

$$\overline{\rho_d \frac{\partial \chi_s}{\partial t}} + \overline{\rho_d \vec{u}} \, \vec{\nabla}\,(\overline{\chi_s}) + \vec{\nabla}\left[\overline{\rho_d}\,\overline{u'\chi'_s}\right] = \overline{S_s} \tag{1.12}$$

This equation states that the source term $\overline{S_s}$ is given by the sum of the rate of change of the mixing ratio χ_s, advection due to spatial gradients in χ_s, and to divergences in the eddy fluxes.

Expanding this in terms of spatial derivatives and assuming constant dry air density give the one point conservation equation of a scalar:

$$\overline{\rho_d \frac{\partial \chi_s}{\partial t}} + \overline{\rho_d u} \frac{\partial \overline{\chi_s}}{\partial x} + \overline{\rho_d v} \frac{\partial \overline{\chi_s}}{\partial y} + \overline{\rho_d w} \frac{\partial \overline{\chi_s}}{\partial z} + \frac{\partial \overline{\rho_d} \overline{u'\chi'_s}}{\partial x} + \frac{\partial \overline{\rho_d} \overline{v'\chi'_s}}{\partial y} + \frac{\partial \overline{\rho_d} \overline{w'\chi'_s}}{\partial z} = \bar{S}_s \tag{1.13}$$

Considering that $\bar{v}$ and $\bar{w}$ are zero, due to axis choice (Sect. 3.2.4) and assuming *horizontal homogeneity* (horizontal gradients nullify) and *steady state conditions* (time derivative nullifies) we get, similar to Eq. 1.10:

$$\frac{\partial \overline{\rho_d w' \chi'}_s}{\partial z} = \bar{S}_s \tag{1.14}$$

expressing that the vertical gradient of eddy covariance is equal to the tracer source/sink term in the volume element. In the case of passive tracers (water vapor, CO_2), this term is zero. In the case of active tracers (ozone, VOCs, $NO_x, \dots$), $\bar{S}_s$ corresponds to the rate of chemical production/destruction of the component in the volume element.

1.3.4   Enthalpy Equation

By replacing ζ by $c_p \theta$, the air enthalpy, one obtains

$$\frac{\partial \rho c_p \theta}{\partial t} + \vec{\nabla}(\vec{u} \rho c_p \theta) = S_\theta \tag{1.15}$$

where c_p is the specific heat of the air and ρ is moist air density. The same development as before leads to

$$\frac{\partial \bar{\theta}}{\partial t} + \bar{u}\frac{\partial \bar{\theta}}{\partial x} + \bar{v}\frac{\partial \bar{\theta}}{\partial y} + \bar{w}\frac{\partial \bar{\theta}}{\partial z} + \frac{\partial \overline{u'\theta'}}{\partial x} + \frac{\partial \overline{v'\theta'}}{\partial y} + \frac{\partial \overline{w'\theta'}}{\partial z} = \frac{1}{\bar{\rho} c_p}\left[\frac{\partial R}{\partial z}\right] \tag{1.16}$$

and

$$\frac{\partial \overline{w'\theta'}}{\partial z} = \frac{1}{\bar{\rho} c_p}\left[\frac{\partial R}{\partial z}\right] \tag{1.17}$$

Where $\frac{\partial R}{\partial z}$ is the vertical radiative flux divergence, which is close to zero in clear surface layers (no fog, rain, smoke, etc.).

1.4   Integrated Relations

Eddy covariance measurements can be used as a tool to estimate fluxes exchanged by ecosystems. To this end, preceding equations may be integrated both horizontally over the area of interest, A $(2L \times 2L)$, and vertically, from soil to the measurement height h_m (Fig. 1.2).
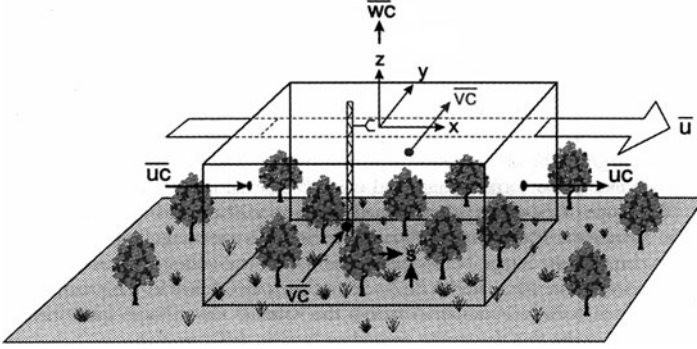
Fig. 1.2 Schematic image of integration of Eq. 1.15 on a control volume in homogeneous terrain (Finnigan et al. 2003)

1.4.1 Dry Air Budget Equation

Integrating Eq. 1.5 on the control volume and assuming horizontal homogeneity gives:

$$\int_0^{h_m} \overline{\frac{\partial \rho_d}{\partial t}} dz + \bar{w}\overline{\rho_d}|_{h_m} + \overline{w'\rho'_d}|_{h_m} = 0 \qquad (1.18)$$

where assumptions of zero flux of dry air at the ground and no net sources or sinks of dry air in the layer of air below h_m are made. Slight imbalances between molar fluxes of CO_2 and O_2 during photosynthesis or respiration or fluxes of nitrogen or volatile organic compounds are extremely small and do not invalidate Eq. 1.18.

1.4.2 Scalar Budget Equation (Generalized Eddy Covariance Method)

Integrating (1.13) in the control volume gives

$$\frac{1}{4L^2} \int_{-L}^{L} \int_{-L}^{L} \int_0^{h_m} \left[\underbrace{\overline{\rho_d}\frac{\partial \overline{\chi_s}}{\partial t}}_{I} + \underbrace{\overline{\rho_d u}\frac{\partial \overline{\chi_s}}{\partial x} + \overline{\rho_d v}\frac{\partial \overline{\chi_s}}{\partial y} + \overline{\rho_d w}\frac{\partial \overline{\chi_s}}{\partial z}}_{II} + \underbrace{\frac{\partial \overline{\rho_d u'\chi'_s}}{\partial x} + \frac{\partial \overline{\rho_d v'\chi'_s}}{\partial y} + \frac{\partial \overline{\rho_d w'\chi'_s}}{\partial z}}_{III \qquad\qquad IV} \right] dz\,dx\,dy$$

$$= \frac{1}{4L^2} \int_{-L}^{L} \int_{-L}^{L} \int_0^{h_m} \underbrace{\overline{S_s}}_{V} dz\,dx\,dy \qquad (1.19)$$

Equation 1.19 represents the complete budget equation of the component s. It shows that the component produced by the source or absorbed by the sink (V)

may be either stored in the control volume (*I*), or transported by advection (*II*), or by turbulence (*III* and *IV*). In these conditions, the source/sink term represents both the sources/sinks inside the air volume and those at the lower limit of the volume (soil, litter).

This equation may be simplified in several ways using different hypotheses. The most common simplification, thoroughly discussed by Finnigan et al. (2003), supposes that the measurement system is placed in a horizontally homogeneous equilibrium layer where all horizontal gradients in Eq. 1.19 are negligible and the mixing ratios and turbulent fluxes measured on the tower are assumed representative of the whole volume. In these conditions, horizontal integration is unnecessary and a simplified one-dimensional mass balance can then be deduced as

$$\underbrace{\int_0^{h_m} \overline{\rho_d} \overline{\frac{\partial \chi_s}{\partial t}} dz}_{I} + \underbrace{\int_0^{h_m} \overline{\rho_d w} \, \overline{\frac{\partial \chi_s}{\partial z}} \, dz}_{II} + \underbrace{\overline{\rho_d} \overline{w' \chi'_s}\big|_{h_m}}_{IV} = \underbrace{F_s}_{V} \tag{1.20}$$

where $\overline{w' \chi'_s}\big|_{h_m}$ represents the vertical turbulent flux at the top of the control volume and F_s the averaged source/sink strength in the whole control volume, that is, the *net ecosystem exchange for the component s*. Term *II* represents the vertical advection at the top of the control volume that results from dry air density change with time in the air layer below h_m. By application of the dry air conservation Eq. 1.18, this term may be rewritten as

$$\int_0^{h_m} \overline{\rho_d w} \, \overline{\frac{\partial \chi_s}{\partial z}} \, dz = - \int_0^{h_m} \left[\int_0^z \overline{\frac{\partial \rho_d}{\partial t}} dz' \right] \overline{\frac{\partial \chi_s}{\partial z}} \, dz \tag{1.21}$$

and after integration by parts as

$$\int_0^{h_m} \overline{\rho_d w} \, \overline{\frac{\partial \chi_s}{\partial z}} \, dz = \int_0^{h_m} [\overline{\chi_s}(z) - \overline{\chi_s}(h)] \overline{\frac{\partial \rho_d}{\partial t}} dz \tag{1.22}$$

Equation 1.20 may thus be rewritten as

$$\int_0^{h_m} \overline{\rho_d} \overline{\frac{\partial \chi_s}{\partial t}} dz + \int_0^{h_m} [\overline{\chi_s}(z) - \overline{\chi_s}(h)] \overline{\frac{\partial \rho_d}{\partial t}} dz + \overline{\rho_d} \, \overline{w' \chi'_s}\big|_{h_m} = F_s \tag{1.23}$$

However, most often, term II is negligible so that Eq. 1.20 may be written more simply as

$$\underbrace{\int_0^{h_m} \overline{\rho_d} \overline{\frac{\partial \chi_s}{\partial t}} dz}_{I} + \underbrace{\overline{\rho_d} \, \overline{w' \chi'_s}\big|_{h_m}}_{IV} = \underbrace{F_s}_{V} \tag{1.24a}$$

This equation is at the basis of the *generalized eddy covariance method*: it suggests indeed that the flux of a scalar exchanged by an ecosystem (F_s, term V) can be estimated as the sum of the vertical eddy covariance $\overline{w'\chi'_s}\big|$ at height h_m (F_s^{EC}, term IV) and of the change of storage of the scalar between the soil and this height (F_s^{STO}, term I), namely:

$$F_s = F_s^{EC} + F_s^{STO} \tag{1.24b}$$

The above hypotheses are known to work fairly well in daytime conditions when turbulence is fully developed, but they appear to be too restrictive to describe completely nighttime conditions. It is then necessary to include the horizontal and vertical advection terms in the conservation equation, with the additional assumption that the vertical integral of $\overline{\rho_d w}\,\partial\overline{\chi}_s/\partial z$ as measured on a single tower is representative of the whole volume. Equation 1.19 then becomes

$$\underbrace{\int_0^{h_m} \bar{\rho}_d \frac{\overline{\partial \chi_s}}{\partial t} dz}_{I} + \underbrace{\int_0^{h_m} \left[\overline{\rho_d w}\frac{\overline{\partial \chi_s}}{\partial z}dz\right]}_{IIa} + \underbrace{\int_0^{h_m} \left[\overline{\rho_d u}\frac{\Delta \bar{\chi}_{s,x}}{\Delta x} + \overline{\rho_d v}\frac{\Delta \bar{\chi}_{s,y}}{\Delta y}\right]dz}_{IIb} + \underbrace{\overline{\rho_d w'\chi'_s}\,\big|_{h_m}}_{IV} = \underbrace{F_s}_{V} \tag{1.25a}$$

in which $\Delta\overline{\chi}_{s,x} = \overline{\chi}_{s,x=L} - \overline{\chi}_{s,x=-L}$ is the difference in mixing ratios at height z between the downwind ($+L$) and upwind ($-L$) vertical planes normal to the x-direction, with a similar definition for $\Delta\overline{\chi}_{s,y}$ in the y-direction. Equation 1.25a may be rewritten as

$$F_s = F_s^{EC} + F_s^{VA} + F_s^{HA} + F_s^{STO} \tag{1.25b}$$

where F_s^{VA} and F_s^{HA} represent vertical (Term IIa) and horizontal (Term IIb) advection of component s. One problem is that these terms cannot be measured on a single tower, and full use of this equation requires a three-dimensional array of instrumentation. The importance of the different terms of this equation will be discussed in Chap. 5.

1.5 Spectral Analysis

Thorough eddy covariance analysis, application of data quality criteria, or correct assessment of some correction factors require a spectral analysis of the (co)variances. The aim of this section is to give the necessary information about spectral analysis of a signal, atmospheric turbulence (co)spectra and the effects of measurement on these (co)spectra to allow the reader to perform these analyses. More details on spectral analysis can be found in the textbooks of Stull (1988), Kaimal and Finnigan (1994), or Foken (2008).

1.5.1 Spectral Analysis of Turbulence

Any turbulent flow may be thought of as a superposition of eddies over a wide range of sizes. As a result, the fluctuation with time of the signals (velocity components, temperature, scalar densities) measured by sensors placed in such flow vary over a wide range of frequencies. The relation between spatial and temporal scale can be established thanks to Taylor's frozen turbulence hypothesis (Taylor 1938) which assumes that eddies do not change significantly in size when convected by the mean wind past a fixed observer. Spectral analysis uses signal frequency decomposition. It is performed by applying an integral transformation which converts a function of time into a function of frequency (f [Hz]):

$$F_s(f) = \frac{1}{\sqrt{2}} \int_{-\infty}^{\infty} \chi_s(t) e^{ift} dt \tag{1.26}$$

$\mathcal{F}(f)$ is called the Fourier transform of the signal. Of special interest in eddy covariance are the power spectrum C_{ss} of a signal χ_s and the cospectrum C_{ws} of two signals w and χ_s. The first one is defined as

$$C_{ss}(f) = \mathcal{F}_s(f). \mathcal{F}_s^*(f) \tag{1.27}$$

and the second as the real part of the cross-spectrum, defined as

$$C_{ws}(f) = \mathcal{F}_w(f) \cdot \mathcal{F}_s^*(f) \tag{1.28}$$

where $\mathcal{F}_s^*(f)$ is the complex conjugate of $\mathcal{F}_w(f)$. $C_{ss}(f)$ and $C_{ws}(f)$ are the spectral and cospectral density, respectively. The main interest of (co) spectra is that their integral over the whole frequency range equals the (co)variance of the signals:

$$\int_0^{\infty} C_{ss}(f) df = \sigma_s^2$$

$$\int_0^{\infty} C_{ws}(f) df = \overline{w' \chi'}_s \tag{1.29}$$

so that (co) spectra may be thought of as a distribution of (co)variances into the different frequency bands of width df.

1.5.2 Spectral Analysis of Atmospheric Turbulence

In the frequency range of interest to micrometeorology, turbulence spectra can be divided into three major spectral regions: (1) at low frequencies (typically 10^{-4} Hz) is the energy containing range, where turbulent energy is produced; (2) at intermediate
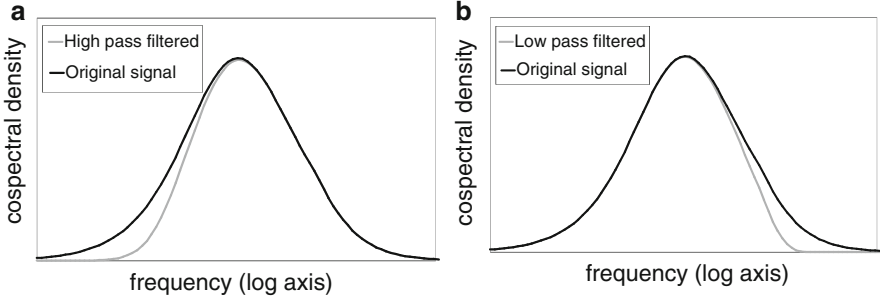
Fig. 1.3 Typical atmospheric cospectrum (*black curve*) with effects of high pass filtering (**a**, *gray curve*) and low pass filtering (**b**, *gray curve*)

frequencies is the inertial subrange, where energy is neither produced nor dissipated but is transformed to smaller and smaller eddies due to an "energy cascade" process (see, e.g. Stull 1988); and (3) at higher frequencies is the dissipation range where turbulent energy is dissipated through viscosity. By considering similarity arguments, one can deduce that the shapes of suitably normalized atmospheric (co)spectra are repeatable and can be described by universal relations. Parameterizations of the momentum and sensible heat cospectra proposed by Kaimal et al. (1972) are given by

$$-\frac{f\,C_{\mathrm{uw}}(f)}{u_*^2} = \frac{12n}{(1+9.6n)^{\frac{7}{3}}} \tag{1.30a}$$

$$-\frac{f\,C_{w\theta}(f)}{u_*\,\theta_*} = \frac{11n}{(1+13.3n)^{\frac{7}{4}}} \quad \text{for} \quad n \leq 1$$

$$-\frac{f\,C_{w\theta}(f)}{u_*\,\theta_*} = \frac{4n}{(1+3.8n)^{\frac{7}{3}}} \quad \text{for} \quad n \geq 1 \tag{1.30b}$$

where n is a dimensionless frequency defined as: $n = f(h_{\mathrm{m}} - d)/\overline{u}$ and d is the zero-plane displacement height. The $\overline{u'w'}$ and $\overline{w'\theta'}$ covariances are normalized by u_*^2 and $u_*\theta_*$, respectively, where u_* is the friction velocity and θ_* is the dynamic temperature. An illustration of Eq. 1.30 is given in Fig. 1.3 (black curve).

1.5.3 Sensor Filtering

Eddy covariance systems, like any sensor, act as frequency filters in dampening high and low frequencies. The reasons for this may be diverse and will be discussed in detail in Sect. 4.1.3. In this chapter, we limit ourselves to the description of

the impact of low or high frequency filtering on the (co)spectra shape and on the resulting error that affects fluxes. The evolution of this impact with measurement height and wind velocity will also be discussed.

To represent high or low frequency dampening by a measurement system, signal theory generally use sigmoidal transfer functions which are equal to 1 in the frequency range where the signal is not attenuated and that decays to zero in the range where signal is attenuated. The shapes of these functions vary according to the processes that are responsible of the dampening (Sect. 4.1.3).

As an example, Fig. 1.3 depict the impact of filtering on a typical cospectrum, Fig. 1.3a showing the effect of a low pass filtering and Fig. 1.3b the effect of a high pass filtering.

The relative error on the fluxes due to frequency losses, $\frac{\delta_s}{F_s^{EC}}$, may be computed according to:

$$\frac{\delta_s}{F_s^{EC}} = 1 - \frac{\int_0^\infty C_{ws}(f) T_{ws}(f) df}{\int_0^\infty C_{ws}(f) df} \tag{1.31}$$

where $C_{ws}(f)$ is the ideal cospectral density and $T_{ws}(f)$ is the apparatus transfer function. The ratio in the integrals on the right hand side of Eq. 1.31 is represented in Fig. 1.3 by the ratio of areas below the gray and black curves. Figure 1.3a shows clearly that low pass filtering causes a loss of covariance and always induces a systematic error. Figure 1.3b suggests the same thing for high pass filtering. However, it could be deceptive as the low frequency spectral range (energy containing range) is not so well defined as it could also depend on mesoscale atmospheric movements. In some conditions, it is possible to observe cospectral densities of different signs at low and high frequencies. In these conditions, the impact of the low pass filtering is not necessarily systematic.

1.5.4 Impacts of Measurement Height and Wind Velocity

The preceding observations allow predicting the impact of measurement height and of wind velocity on errors due to frequency losses, which is synthesized in Fig. 1.4.

Equations 1.30 describe universal cospectra as functions of the nondimensional frequency $n = \frac{f(h_m - d)}{\bar{u}}$. This implies that the decrease in $h_m - d$ shifts the cospectrum toward higher frequencies (Fig. 1.4). However, as the apparatus transfer function does not depend on measurement height, systems placed at lower heights would be more sensitive to high-frequency losses (Fig. 1.4a) while systems placed at higher heights would be more sensitive to low-frequency losses (Fig. 1.4b). The first ones would require set ups able to capture fluctuations at higher frequencies while the second would need longer averaging times (the main cause of low-frequency losses). Further details about frequency losses and their correction are presented in Sect. 4.1.3.
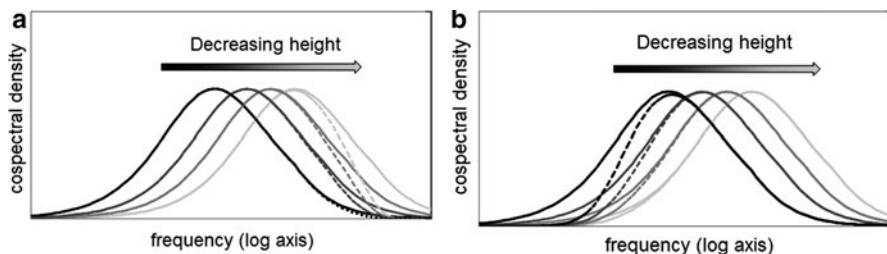
Fig. 1.4 (**a**) Undamped (*full line*) and low pass filtered (*dotted line*) cospectra; (**b**) Undamped (*full line*) and high pass filtered (*dotted line*) cospectra

References

André J-C, Bougeault P, Goutorbe J-P (1990) Regional estimates of heat and evaporation fluxes over non-homogeneous terrain, Examples from the HAPEX-MOBILHY programme. Bound Layer Meteorol 50:77–108

Aubinet M, Grelle A, Ibrom A, Rannik Ü, Moncrieff J, Foken T, Kowalski AS, Martin PH, Berbigier P, Bernhofer C, Clement R, Elbers J, Granier A, Grünwald T, Morgenstern K, Pilegaard K, Rebmann C, Snijders W, Valentini R, Vesala T (2000) Estimates of the annual net carbon and water exchange of forests: the EUROFLUX methodology. Adv Ecol Res 30: 113–175

Baldocchi D, Falge E, Gu L, Olson R, Hollinger D, Running S, Anthoni P, Bernhofer C, Davis K, Evans R, Fuentes J, Goldstein A, Katul G, Law B, Lee X, Malhi Y, Meyers T, Munger W, Oechel W, PawU KT, Pilegaard K, Schmid HP, Valentini R, Verma S, Vesala T (2001) FLUXNET: a new tool to study the temporal and spatial variability of ecosystem-scale carbon dioxide, water vapor, and energy flux densities. Bull Am Meteorol Soc 82:2415–2434

Barrett EW, Suomi VE (1949) Preliminary report on temperature measurement by sonic means. J Meteorol 6:273–276

Boussinesq J (1877) Essai sur la théorie des eaux courantes. Mem Savants Etrange 23, 46 pp

Bovscheverov VM, Voronov VP (1960) Akustitscheskii fljuger (Acoustic rotor). Izv AN SSSR Ser Geofiz 6:882–885

Brutsaert W (1982) Evaporation into the atmosphere. D. Reidel Publ. Co., Dordrecht, 299 pp

Buck AL (1973) Development of an improved Lyman-alpha hygrometer. Atmos Technol 2:213–240

Businger JA (1982) Equations and concepts. In: Nieuwstadt FTM, Van Dop H (eds) Atmospheric turbulence and air pollution modelling: a course held in The Hague, 21–25 September 1981. D. Reidel Publ. Co., Dordrecht, pp 1–36

Businger JA, Oncley SP (1990) Flux measurement with conditional sampling. J Atmos Ocean Technol 7:349–352

Coppin PA, Taylor KJ (1983) A three component sonic anemometer/thermometer system for general micrometeorological research. Bound Layer Meteorol 27:27–42

Desjardins RL (1977) Description and evaluation of a sensible heat flux detector. Bound Layer Meteorol 11:147–154

Elagina LG (1962) Optitscheskij pribor dlja izmerenija turbulentnych pulsacii vlaschnosti (Optical sensor for the measurement of turbulent humidity fluctuations). Izv AN SSSR, ser Geofiz. 12:1100–1107

Elagina LG, Lazarev AI (1984) Izmerenija tschastotnych spektrov turbulentnych pulsacij CO_2 v prizemnom sloje atmosphery (Measurement of the turbulence spectra of CO_2 in the atmospheric surface layer). Izv AN SSSR Fiz Atm Okeana 20:536–540

Falge E, Baldocchi D, Olson R, Anthoni P, Aubinet M, Bernhofer C, Burba G, Ceulemans R, Clement R, Dolman H, Granier A, Gross P, Grunwald T, Hollinger D, Jensen NO, Katul G, Keronen P, Kowalski A, Lai CT, Law BE, Meyers T, Moncrieff H, Moors E, Munger JW, Pilegaard K, Rannik U, Rebmann C, Suyker A, Tenhunen J, Tu K, Verma S, Vesala T, Wilson K, Wofsy S (2001a) Gap filling strategies for long term energy flux data sets. Agric For Meteorol 107:71–77

Falge E, Baldocchi D, Olson R, Anthoni P, Aubinet M, Bernhofer C, Burba G, Ceulemans R, Clement R, Dolman H, Granier A, Gross P, Grunwald T, Hollinger D, Jensen NO, Katul G, Keronen P, Kowalski A, Lai CT, Law BE, Meyers T, Moncrieff H, Moors E, Munger JW, Pilegaard K, Rannik U, Rebmann C, Suyker A, Tenhunen J, Tu K, Verma S, Vesala T, Wilson K, Wofsy S (2001b) Gap filling strategies for defensible annual sums of net ecosystem exchange. Agric For Meteorol 107:43–69

Finnigan JJ, Clement R, Malhi Y, Leuning R, Cleugh HA (2003) A re-evaluation of long-term flux measurement techniques, Part I: averaging and coordinate rotation. Bound Layer Meteorol 107:1–48

Foken T (2008) Micrometeorology. Springer, Berlin/Heidelberg, 308 pp

Foken T, Dlugi R, Kramm G (1995) On the determination of dry deposition and emission of gaseous compounds at the biosphere-atmosphere interface. Meteorol Z 4:91–118

Foken T, Oncley SP (1995) Results of the workshop 'Instrumental and methodical problems of land surface flux measurements'. Bull Am Meteorol Soc 76:1191–1193

Foken T, Wichura B (1996) Tools for quality assessment of surface-based flux measurements. Agric For Meteorol 78:83–105

Garratt JR (1992) The atmospheric boundary layer. Cambridge University Press, Cambridge, 316 pp

Gash JHC (1986) A note on estimating the effect of a limited fetch on micrometeorological evaporation measurements. Bound Layer Meteorol 35:409–414

Gerosa G, Cieslik S, Ballarin-Denti A (2003) Ozone dose to a wheat field determined by the micrometeorological approach. Atmos Environ 37:777–788

Güsten H, Heinrich G (1996) On-line measurements of ozone surface fluxes: Part I: methodology and instrumentation. Atmos Environ 30:897–909

Hanafusa T, Fujitana T, Kobori Y, Mitsuta Y (1982) A new type sonic anemometer-thermometer for field operation. Pap Meteorol Geophys 33:1–19

Hargreaves KJ, Fowler D, Pitcairn CER, Aurela M (2001) Annual methane emission from Finnish mires estimated form eddy co-variance campaign measurements. Theor Appl Climatol 70: 203–213

Horst TW, Weil JC (1994) How far is far enough?: The fetch requirements for micrometeorological measurement of surface fluxes. J Atmos Ocean Technol 11:1018–1025

Hyson P, Hicks BB (1975) A single-beam infrared hygrometer for evaporation measurement. J Appl Meteorol 14:301–307

Kaimal JC, Businger JA (1963) A continuous wave sonic anemometer-thermometer. J Clim Appl Meteorol 2:156–164

Kaimal JC, Finnigan JJ (1994) Atmospheric boundary layer flows: their structure and measurement. Oxford University Press, Oxford, 289 pp

Kaimal JC, Wyngaard JC, Izumi Y, Coté OR (1972) Spectral characteristics of surface layer turbulence. Q J R Meteorol Soc 98:563–589

Karl TG, Spirig C, Rinne J, Stroud C, Prevost P, Greenberg J, Fall R, Guenther A (2002) Virtual disjunct eddy covariance measurements of organic compound fluxes from a subalpine forest using proton transfer reaction mass spectrometry. Atmos Chem Phys 2:279–291

Kowalski AS, Serrano-Ortiz P (2007) On the relationship between the eddy covariance, the turbulent flux, and surface exchange for a trace gas such as CO_2. Bound Layer Meteorol 124:129–141

Kretschmer SI, Karpovitsch JV (1973) Maloinercionnyj ultrafioletovyj vlagometer (Sensitive ultraviolet hygrometer). Izv AN SSSR Fiz Atm Okeana 9:642–645

Kroon PS, Hensen A, Jonker HJJ, Ouwersloot HG, Vermeulen AT, Bosveld FC (2010) Uncertainties in eddy covariance flux measurements assessed from CH4 and N2O observations. Agric For Meteorol 150:806–816

Lamaud E, Brunet Y, Labatut A, Lopez A, Fontan J, Druilhet A (1994) The Landes experiment: biosphere–atmosphere exchanges of ozone and aerosol particles, above a pine forest. J Geophys Res 99:16511–16521

Laville P, Jambert C, Cellier P, Delmas R (1999) Nitrous oxide fluxes from a fertilized maize crop using micrometeorological and chamber methods. Agric For Meteorol 96:19–38

Lee X (1998) On micrometeorological observations of surface-air exchange over tall vegetation. Agric For Meteorol 91:39–49

Lenschow DH, Mann J, Kristensen L (1994) How long is long enough when measuring fluxes and other turbulence statistics? J Atmos Ocean Technol 11:661–673

Lettau HH, Davidson B (eds) (1957) Exploring the atmosphere's first mile, vol 1. Pergamon Press, London/New York, 376 pp

Leuning RL (2003) Measurements of trace gas fluxes in the atmosphere using eddy covariance: WPL corrections revisited. In: Lee X et al (eds) Handbook of micrometeorology. Kluwer Academic, Dordrecht/Boston/London, pp 119–132

Leuning R (2007) The correct form of the Webb, Pearman and Leuning equation for eddy fluxes of trace gases in steady and non-steady state, horizontally homogeneous flows. Bound Layer Meteorol 123:263–267

Leuning RL, Moncrieff JB (1990) Eddy covariance CO_2 flux measurements using open and closed path CO_2 analysers: correction for analyser water vapour sensitivity and damping of fluctuations in air sampling tubes. Bound Layer Meteorol 53:63–76

Martini L, Stark B, Hunsalz G (1973) Elektronisches Lyman-Alpha-Feuchtigkeitsmessgerät. Z Meteorol 23:313–322

McBean GA (1972) Instrument requirements for eddy correlation measurements. J Appl Meteorol 11:1078–1084

McMillen RT (1988) An eddy correlation technique with extended applicability to non-simple terrain. Bound Layer Meteorol 43:231–245

Mitsuta Y (1966) Sonic anemometer-thermometer for general use. J Meteorol Soc Jpn Ser II 44:12–24

Moncrieff J (2004) Surface turbulent fluxes. In: Kabat P et al (eds) Vegetation, water, humans and the climate. A new perspective on an interactive system. Springer, Berlin/Heidelberg, pp 173–182

Moncrieff JB, Massheder JM, DeBruin H, Elbers J, Friborg T, Heusinkveld B, Kabat P, Scott S, Søgaard H, Verhoef A (1997a) A system to measure surface fluxes of momentum, sensible heat, water vapor and carbon dioxide. J Hydrol 188–189:589–611

Moncrieff JB, Valentini R, Greco S, Seufert G, Ciccioli P (1997b) Trace gas exchange over terrestrial ecosystems: methods and perspectives in micrometeorology. J Exp Bot 48:1133–1142

Montgomery RB (1948) Vertical eddy flux of heat in the atmosphere. J Meteorol 5:265–274

Moore CJ (1986) Frequency response corrections for eddy correlation systems. Bound Layer Meteorol 37:17–35

Obukhov AM (1951) Charakteristiki mikrostruktury vetra v prizemnom sloje atmosfery (Characteristics of the micro-structure of the wind in the surface layer of the atmosphere). Izv AN SSSR ser Geofiz 3:49–68

Ohtaki E, Matsui T (1982) Infrared device for simultaneous measurement of fluctuations of atmospheric carbon dioxide and water vapor. Bound Layer Meteorol 24:109–119

Raupach MR (1978) Infrared fluctuation hygrometer in the atmospheric surface layer. Q J R Meteorol Soc 104:309–322

Schmid HP, Oke TR (1990) A model to estimate the source area contributing to turbulent exchange in the surface layer over patchy terrain. Q J R Meteorol Soc 116:965–988

Schotanus P, Nieuwstadt FTM, DeBruin HAR (1983) Temperature measurement with a sonic anemometer and its application to heat and moisture fluctuations. Bound Layer Meteorol 26:81–93

Schotland RM (1955) The measurement of wind velocity by sonic waves. J Meteorol 12: 386–390

Schuepp PH, Leclerc MY, MacPherson JI, Desjardins RL (1990) Footprint prediction of scalar fluxes from analytical solutions of the diffusion equation. Bound Layer Meteorol 50:355–373

Sellers PJ, Hall FG, Asrar G, Strebel DE, Murphy RE (1988) The first ISLSCP field experiment (FIFE). Bull Am Meteorol Soc 69:22–27

Smith KA, Clayton H, Arah JRM, Christensen S, Ambus P, Fowler D, Hargreaves KJ, Skiba U, Harris GW, Wienhold FG, Klemedtsson L, Galle B (1994) Micrometeorological and chamber methods for measurement of nitrous oxide fluxes between soils and the atmosphere: overview and conclusions. J Geophys Res 99:16541–16548

Spirig C, Neftel A, Ammann C, Dommen J, Grabmer W, Thielmann A, Schaub A, Beauchamp J, Wisthaler A, Hansel A (2005) Eddy covariance flux measurements of biogenic VOCs during ECHO 2003 using proton transfer reaction mass spectrometry. Atmos Chem Phys 5:465–481

Stull RB (1988) An Introduction to boundary layer meteorology. Kluwer Academic, Dordrecht/Boston/London, 666 pp

Suomi VE (1957) Sonic anemometer – University of Wisconsin. In: Lettau HH, Davidson B (eds) Exploring the atmosphere's first mile. Pergamon Press, London/New York, pp 256–266

Swinbank WC (1951) The measurement of vertical transfer of heat and water vapor by eddies in the lower atmosphere. J Meteorol 8:135–145

Taylor GI (1938) The spectrum of turbulence. Proc R Soc Lond A164(919):476–490

Tsvang LR, Fedorov MM, Kader BA, Zubkovskii SL, Foken T, Richter SH, Zelený J (1991) Turbulent exchange over a surface with chessboard-type inhomogeneities. Bound Layer Meteorol 55:141–160

Vickers D, Mahrt L (1997) Quality control and flux sampling problems for tower and aircraft data. J Atmos Ocean Technol 14:512–526

Webb EK, Pearman GI, Leuning R (1980) Correction of the flux measurements for density effects due to heat and water vapour transfer. Q J R Meteorol Soc 106:85–100

Zhang SF, Wyngaard JC, Businger JA, Oncley SP (1986) Response characteristics of the U.W. sonic anemometer. J Atmos Ocean Technol 2:548–558